Method for modeling transport of particles in realistic porous networks: Application to the computation of NMR flow propagators

Guillemette Picard
Schlumberger Doll Research, 1 Hampshire street, Cambridge, Massachusetts 02139, USA

Kurt Frey
Department of Chemical Engineering, Massachusetts Institute of Technology, 77 Massachusetts Avenue, Cambridge, Massachusetts 02139-4307, USA

(Received 13 March 2007; published 22 June 2007)

We model the transport of particles present in a fluid steadily flowing through a porous medium. The porous medium is described by a representative three-dimensional network. The particles are subjected to advection by the flow and to thermal diffusion. We propose to calculate their trajectories with the continuous time random walk framework. This enables us to efficiently sample disordered networks with realistic topology. The method proposed in this paper is general and can be adapted to model dispersion of tracers. It is applied here to simulate the measurement of the flow propagator $P(\underline{x}, \delta t)$ which is defined as the ensemble density distribution of tracer displacements $\underline{x}$, in a given time interval δt. It can be extracted from pulsed magnetic field gradient spin echo NMR experiments carried out on porous media while fluid is flowing. Preliminary numerical results show good qualitative agreement with experiments.

DOI: 10.1103/PhysRevE.75.066311 PACS number(s): 47.56.+r, 47.27.eb, 91.60.Tn

I. INTRODUCTION

Characterization of the transport of a passive tracer when it is injected into a fluid flowing in a porous medium remains a scientific challenge. Its dispersion depends on the structure of the porous medium in a complex way. This question has applications in various fields like the migration of contaminants in groundwater systems, miscible displacement in enhanced petroleum recovery, chromatography, and so on. One of the difficulties is the imaging of the tracer in the medium. In the last decade, there has been an increasing body of experiments reporting characterization of flow in rock samples with NMR techniques that could help in understanding dispersion in such porous media. While fluid is steadily flowing, pulsed field gradient NMR is used to tag the positions of the fluid's polarized protons at an initial time t_0 and to then obtain the density distribution $P(\underline{x}, \delta t)$ for the displacement $\underline{x}$ of the spins at a later time $t_0+\delta t$ [1–8]. The density distribution of the displacement of spins submitted to advection by the flow and molecular diffusion is named the flow propagator. For single-phase flows, the flow propagator carries the signature of the connected structure of the porous medium. While the experimental techniques are rapidly developing with, for instance, two-phase flow propagators [9], the interpretation of the single-phase flow propagator is still preliminary.

Computing the flow propagator raises issues similar to those in the modeling of hydrodynamic front dispersion in porous media. Only the initial conditions differ. In the first case, particles are uniformly distributed in the fluid, while in the second case they are initially organized as a front or locally distributed patch. The physics of the transport is then the same. Thus modeling the flow propagator benefits from the activity in research dealing with the description the dispersion of tracer particles [10–12].

Several approaches have been proposed to describe the advection-diffusion of passive tracer particles in porous media. We focus here on network models for porous media [13–16]. Modeling the pore space with a network of nodes and bonds enables a numerically efficient calculation of the flow properties. The particles submitted to advection and diffusion are then tracked in the network [17–21]. An interesting review of dispersion in network models can be found in [22]. Most of these simulations have been done using regular networks and standard random walkers. If networks are disordered or heterogeneous, these methods can be extremely costly in terms of computing time, in particular because random walkers can be trapped in slow flow regions or dead ends.

Following an approach proposed by several groups, [22–24], we use the continuous time random walk framework so as to track particles hopping from node to node in disordered networks. Other researchers have used this method to model front dispersion in regular lattices [25,26]. The specificity of the work presented here is threefold: (i) A semianalytical expression of the hopping time distribution is developed which considerably reduces computing time. (ii) The node to node tracking algorithm is embedded into a general model adaptable to any network and particles transport. Refinements to the simple model presented here are proposed if they are needed by specific problems. (iii) The general algorithm is applied to the calculation of the flow propagator. Thus we combine the use of porous network and continuous time random walks to efficiently numerically model general dispersion problems in heterogeneous porous media.

In the next section we present a general model for particle tracking in disordered networks. The third section presents an application to the calculation of the flow propagator in a realistic network with a topology extracted from a Berea sandstone [14]. The last section is devoted to discussion of the validity of the model and conclusions.

II. AN EFFICIENT MODEL FOR ADVECTION DIFFUSION IN POROUS NETWORKS

A. Porous networks with a realistic topology

Networks model the porous space of a porous medium with an ensemble of nodes connected with bonds. The topology of the network can be as simple as a regular lattice, where the bonds have a fixed length, and set orientations. Alternatively, it can be disordered with a distribution of bond lengths, orientations, cross sections, as well as a distribution of nodes coordination numbers. Several methods are currently applied to derive a realistic topology from a rock sample. The topology of the porous space is extracted from two-dimensional thin sections combined with numerical modeling of geological processes [14,15,27] or from three-dimensional microtomographic images of the rock samples [13,16]. There is currently an important effort towards the extraction and validation of consistent networks. This discussion is beyond the scope of this paper, and we will focus on a network already processed by Bakke and Oeren [14] with a topology representative of a Berea sandstone.

The flow in every bond is classically calculated in porous network models in the following way: a macroscopic pressure difference is applied between the inlet and the outlet faces of the network. Poiseuille flow is assumed in every bond. The conservation of flow at every node gives a linear system of equations. Solving the system provides the nodal pressures. By simply rescaling the macroscopic pressure difference, the network average flow velocity is rescaled to any desired value.

As a first approach in our particle tracking algorithm, the flow in every bond is approximated with a mean velocity. This one-dimensional description of the flow in every bond enables us to have a semianalytical model. The limits of this assumption are detailed in the last section.

B. Node to node tracking of particles

Once the mean velocity in every bond is known, particles are tracked in the network. Between nodes, they move because of advection and thermal diffusion. The crossing of a bond is described as a hop from one node to a neighboring one with a distribution of times calculated for each bond. In the following section, we present an exact calculation of the first arrival time distribution [22,23,28,29].

A central assumption is the complete mixing at the nodes: a particle at node i is transported to a neighboring node j independently of the last crossed bond. The nodes are considered volumeless, that is, no time is spent in the nodes. The validity of these assumptions is discussed in the last section.

We consider a lattice network of nodes i connected to z bonds ij of cross section S_{ij} and length l_{ij}. The mean velocity u_{ij} is calculated in every bond as described previously. Let $c_{ij}(x_{ij},t)$ be the particle concentration in the bond ij. It satisfies the one-dimensional advection-diffusion equation

$$\partial_t c_{ij} + u_{ij}\partial_x c_{ij} = D\partial_{xx}^2 c_{ij}, \tag{1}$$

where D is the molecular diffusion.

The quantity describing the transport is the first arrival time distribution (FATD) $p_{ij}(t)$, that is, the probability for the particle leaving node i to first reach node j after a time t.

In order to derive the FATD from the concentration for a node i, one has to solve for all the equations Eq. (1) for the z bonds ij originating from i with the boundary conditions [23,29]

$$c_{ij}(l_{ij},t) = 0, \quad \text{for } j = 1,z, \tag{2}$$

$$c_{ij}(0,t) = \xi_i(t) \quad \text{for } j = 1,z, \tag{3}$$

$$\sum_{j=1}^{z} S_{ij}(u_{ij}c_{ij} - D\partial_x c_{ij}) = \delta(t). \tag{4}$$

The condition Eq. (3) imposes the same concentration ξ_i at the onset of the bonds connected to node i. The condition Eq. (4) indicates that a particle leaves node i at time $t=0$. The summation is over the z bonds connected to the node i. Thus, the probability to first arrive at node j is the flux

$$p_{ij}(t) = S_{ij}(u_{ij}c_{ij} - D\partial_x c_{ij})(l_{ij},t) = -S_{ij}D\partial_x c_{ij}(l_{ij},t).$$

The system consisting of Eq. (1) with the boundary conditions Eqs. (2)–(4) is solved in the Laplace domain. The Laplace transform of $c_{ij}(t)$ is denoted $\tilde{c}_{ij}(x,s)$. Thus, z second order ordinary differential equations for the Laplace transform concentrations $\tilde{c}_{ij}(x,s)$ are obtained. The general solution is

$$\tilde{c}_{ij}(x,s) = A_{ij}e^{\alpha_{ij}x} + B_{ij}e^{\beta_{ij}x},$$

$$\text{with } \alpha_{ij},\beta_{ij} = (1/2D)(u_{ij} \pm \sqrt{u_{ij}^2 + 4Ds}) \tag{5}$$

where the $2z$ coefficient can be determined from the boundary conditions Eqs. (2)–(4). After several steps, the Laplace transform of $p_{ij}(t)$ is expressed as

$$\tilde{p}_{ij}(s) = S_{ij}D\tilde{\xi}_i(s)\frac{\beta_{ij} - \alpha_{ij}}{e^{-\alpha_{ij}l_{ij}} - e^{-\beta_{ij}l_{ij}}},$$

$$\tilde{\xi}_i^{-1}(s) = D\sum_{j=1}^{z} S_{ij}\frac{\beta_{ij}e^{\beta_{ij}l_{ij}} - \alpha_{ij}e^{\alpha_{ij}l_{ij}}}{e^{\beta_{ij}l_{ij}} - e^{\alpha_{ij}l_{ij}}}. \tag{6}$$

The cumulative probability distribution $P_{ij}(s)$ is the probability to exit via bond ij. It can be calculated by integrating $p_{ij}(t)$ over all times, or with the Laplace transforms $\tilde{P}_{ij}(s) = p_{ij}(s)/s$. The latter relation is used, and with the final value theorem, we obtain an expression for the the probability to exit via throat ij:

$$P_{ij} = \frac{S_{ij}}{\sum_k S_{ik}u_{ik}\dfrac{1}{1-e^{-\wp_{ik}}}}\frac{u_{ij}}{1-e^{-\wp_{ij}}}, \tag{7}$$

where the Péclet numbers were introduced as $\wp_{ij} = u_{ij}l_{ij}/D$. It is checked that limit behaviors are consistent. (i) In the convective limit ($u_{ik} \to \infty$ for all k, that is, $\wp_{ik} \gg 1$), the probability to exit via bond ij described by Eq. (7) is

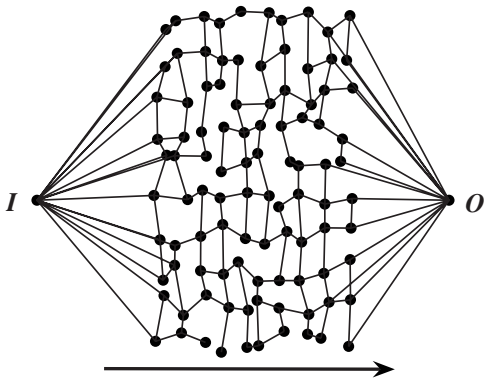

FIG. 1. Schematic two-dimensional description of the network. The network has $N_{nodes}+2$ nodes. On the inlet and outlet faces, the nodes are connected to an inlet node and an outlet node. Note that this is a schematic representation and the simulations are performed on a three-dimensional network.

$$P_{ij} = \begin{cases} 0 & \text{if } u_{ij} < 0, \\ \dfrac{S_{ij}u_{ij}}{\sum_{k}^{+} S_{ik}u_{ik}} & \text{if } u_{ij} > 0, \end{cases} \tag{8}$$

where the sum Σ_k^+ is only on the links ik with a positive velocity $u_{ik}>0$. Thus when diffusion is negligible, the probability to exit via tube ij is the ratio of the positive flow rate through bond ij to the sum of the total positive flow rates through bonds connected to i. (ii) In the opposite diffusive limit ($u_{ik}\to 0$ for all k, that is, $\wp_{ik}\ll 1$), we find that the probability to exit via tube ij described by Eq. (7) is

$$P_{ij} = \frac{S_{ij}/l_{ij}}{\sum_{k} S_{ik}/l_{ik}} \tag{9}$$

The presence of the lengths of the bonds in this expression is due to the fact that P_{ij} is the probability to exit the bond ij. (The probability to enter the bond ij in the absence of convection would be $P_{ij}^{in}=S_{ij}/\Sigma_k S_{ik}$.)

Thus the model describes the dynamics of particles with hops from one node to a neighboring node. Equation (7) gives the probability to first reach each neighboring node, while Eq. (6) gives the distribution of first arrival times. The continuous time random walk framework avoids the description of the wandering of the particles due to diffusion before they reach nodes. For instance, a particle leaving node i, may wander into bond ik without reaching node k, then go back to node i, and eventually cross bond ij. With this model, its wandering is integrated in the first arrival time distribution $p_{ij}(t)$.

C. Adaptation to front dispersion and flow propagators

The previous section describes the dynamics of a particle first arriving at a node j coming from a node i and is a general tracking algorithm. Specific boundary conditions need to be added at the network scale. Figure 1 is introduced as a schematic two-dimensional representation of the network. The nodes at one end of the network are connected to an inlet node I, and those at the other end are connected to an outlet node O. The total number of internal nodes is denoted N_{nodes}.

Let $n_i(t)$ be the number of particles that first arrive at node i per unit time, and $n_I(t)$ the number of particles that leave the inlet node per unit time. As they are volumeless, there is no accumulation of particles at the internal nodes i: the fluxes of particles J_{ik} through the bonds connected to i are as follows in the Laplace domain:

$$\sum_{k} \tilde{J}_{ik}(s) = \sum_{k} \tilde{p}_{ik}(s)\tilde{n}_i(s) - \tilde{p}_{ki}(s)\tilde{n}_k(s) = 0. \tag{10}$$

Thus, there are N_{nodes} linear equations and $N_{nodes}+1$ unknowns $n_i(t)$ and $n_I(t)$. The closure of the system is chosen depending on the type of dispersion that is modeled.

First, when modeling the dispersion of a tracer front [24,25], the closure of the system describes the pulse input of tracers at the inlet node:

$$\sum_{k} \tilde{J}_{Ik}(s) = 1. \tag{11}$$

The system defined by Eqs. (10) and (11) is a linear system that can be directly solved in the Laplace domain. $\tilde{n_i}(s)$ and $\tilde{n_I}(s)$ can then be inverted in the time domain. This provides a very efficient method to compute front dispersion in disordered networks.

Second, when computing the flow propagator, we model a pulsed magnetic field gradient spin echo NMR experiments, where the spins of the fluid are excited and tracked during a time lapse δt. End effects on the core sample during the experiment are neglected: the volume of fresh fluid without excited spins that enters the core during the time lapse δt does not significantly affect the measurements. Surface relaxation of the spins is also neglected. With these two assumptions, the concentration of excited spins that are detected, that is, that have not relaxed after δt, is constant over time and uniform in the fluid. We model the excited spins with particles hopping from node to node in a network representative of the porous medium. The distribution of particles is kept constant and uniform in the fluid by imposing a constant flux of particles at the inlet:

$$\sum_{k} J_{Ik}(t) = J_I. \tag{12}$$

Note that the number of particles that first arrive per node per unit time, n_i, n_I, will be constant over time.

The system constituted by the N_{nodes} equations (10) and the boundary condition (12) is closed, but cannot be simply solved, as Eqs. (10) are written in the Laplace domain whereas Eq. (12) is written in the time domain.

Thus, instead of directly solving this system, we adopt an equivalent approach: particles are successively tracked in the network in the time domain. They are initially inserted in the nodes with an arbitrary distribution $n_i(t=0)$. The constant flux of particles at the inlet is ensured by reassigning instantaneously every particle that reaches the outlet node, into the inlet node. Within the network, at every node i, the particle is

assigned to a neighboring node j with the cumulated probabilities Eq. (7), and is attributed a time to reach j according the probability law $p_{ij}(t)$. The number of particles per node $n_i(t)$ rapidly converges to constant values of n_i. Once the numerical model has relaxed, the flow propagator is calculated as the probability of displacement in a time lapse δt, as will be shown in the next section.

III. CALCULATION OF THE FLOW PROPAGATORS IN A BEREA-SANDSTONE-LIKE NETWORK

A. Berea sandstone network

The model is applied to a network with a topology extracted from a Berea sandstone and proposed by Oeren and Bakke [14,15,27]. Their original network consists of nodes linked with bonds representative of pores and throats. The bonds have constant cross sections that are circular, rectangular, or triangular. In our numerical model, the volume of the nodes has been canceled, and the bonds have been elongated so as to intersect on volumeless nodes. The topology remains identical. The network used is of cubic shape with 3-mm-long sides. It is composed of 26 146 bonds and $N_{nodes}=12\,349$ nodes with coordination numbers ranging from 1 to 19 with an average value of 4.2. The average length of the bonds is $\langle l_{ij}\rangle=116$ μm and the average value of the equivalent radii $\langle\sqrt{S_{ij}}\rangle=32$ μm.

B. Advection-diffusion of particles in the Berea network

The first step of the model is the calculation of the mean flow velocity in each bond as described in Sec. II A. The calculations are done in this section with a macroscopic pressure difference of 147 Pa corresponding to an average velocity of 0.25 mm/s, and an average Péclet number of 12. The diffusion coefficient is set to $D=2.4\times10^{-9}$ m^2 s^{-1}.

The second step is the calculation of the first arrival time distributions for each bond with the semianalytical expression given in the Appendix. Figure 2 shows the cumulative first arrival time distribution $[\int_0^t p_{ij}(t')dt']$ for the five bonds connected to one given node of the network. Note that, in the absence of diffusion, every cumulative first arrival time distribution would be a step function, occurring at the time needed for transport by the flow, that is, the ratio of the length of the bond to the mean flow velocity in the bond. Here, this parameter still plays a dominant role, and a sharp increase in probability occurs at this value. The fraction of particles going into each bond has a complex dependence on flow rate, cross section, and length of the bond.

The third step of the model is the successive tracking of particles from node to node, until the equilibrium of the model is reached. Then measurements can be performed.

The trajectories of 50 000 particles are successively initiated in the nodes.

Three different initial distributions were tested. The numerical steady state is independent of the initial distribution.

Figure 3 shows the velocity (displacement during 0.1 s divided by 0.1 s) along the flow direction averaged over all the particles versus time. For all the initial distributions tested, after a duration corresponding to 10 s a plateau is

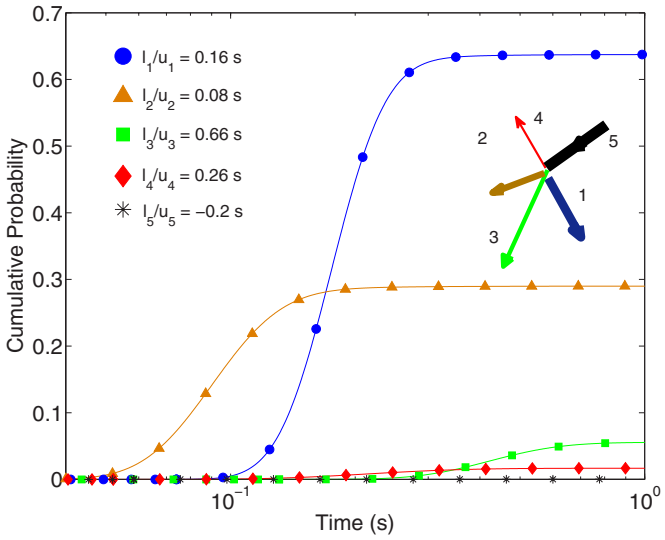

FIG. 2. (Color online) Particles are input in one node of the Berea network schematized in the inset. The mean velocity in the network is 0.25 mm/s. The legend is the convection time, that, is the ratio of the bond length to the bond velocity. The negative time corresponds to a direction of flow entering the node. The cumulative first arrival time distributions to cross the five throats connected to the node are calculated.

reached, showing that the numerical model has relaxed. With the formalism of Sec. II C, this means that the number of particles that first arrive at node i per unit time $n_i(t)$ reached their steady state value n_i. At equilibrium, it is checked that the flux of particles per time unit is a linear function of the flow rate in each bond as expected at steady state for a system with uniform concentration. The linear coefficient 2.4×10^4 particles/mm^3 is the concentration of particles per unit volume (Fig. 4). It is checked that this is equal to the number of particles tracked divided by the total volume of the bonds.

The last step is the calculation of the flow propagator after the numerical relaxation described by Fig. 3 has taken place.

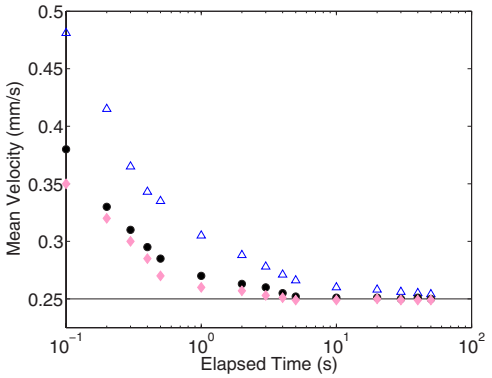

FIG. 3. (Color online) Equilibration of the model: Instantaneous mean velocity averaged over 50 000 particles versus equivalent time. The numerical system converges toward a steady state. The open triangles correspond to an initiation of particles in 500 nodes arbitrarily chosen, the black dots to a random initiation in all the nodes, and the diamonds to an initiation in the nodes according to the summed volume of the connected bonds.

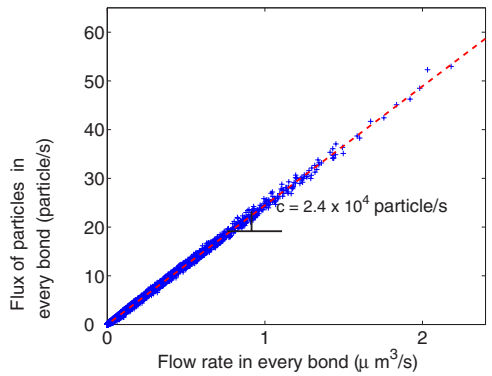

FIG. 4. (Color online) At equilibrium, the flux of particles across a bond ij is a linear function of the flow rate $S_{ij}u_{ij}$. The linear coefficient is the concentration of particles per fluid volume unit, 2.4×10^4 particles/mm^3.

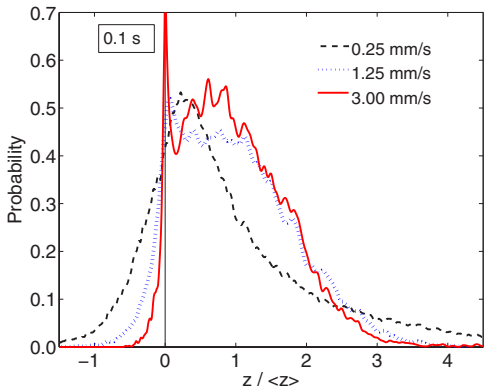

FIG. 5. (Color online) Flow propagator for an average velocity in the network $\langle v\rangle$=0.25, 1.25, and 3 mm/s and a time lapse δt=0.1 s.

C. Flow propagator in the Berea sandstone network

In this section, the results for the calculation of the flow propagator in the network with a realistic topology are presented.

The tracking of the particles is the most computationally intensive part of the algorithm. Thanks to the continuous time random walk framework, the time required for these calculations scales linearly in the number of particles being used, and in the number of nodes visited per particles. The number of particles selected for tracking should be sufficient that the number of node visits after numerical relaxation greatly exceeds the total number of nodes. A higher ratio of node visits to total nodes increases the signal to noise ratio in the resulting flow propagator. At a ratio of 100:1 a simple running average filter is sufficient to eliminate most of the noise. As an example, in the Berea network with 12 349 nodes, the tracking of 10^5 particles for a time corresponding to 2 s after relaxation, at an average velocity of 1.25 mm/s represents an average of about 150 visits per node, and a computation time of the order of 1 h on a single processor. (With simple random walk simulations, the time required for equivalent calculation scales linearly in the number of particles and the number of time steps in every bond per particle. When a particle is trapped in a slow flow zone, the computing time required becomes prohibitive. Thus random walk simulations will be less efficient at dealing with a heterogeneous disordered medium.)

After the numerical relaxation, the trajectory of each particle is recorded as a list of nodes reached and time elapsed for a total duration corresponding to 2 s. In order to avoid an increase in the number of particles required for an accurate calculation, the trajectories of the 10^5 particles recorded for a duration of 2 s are used, and the propagator is calculated as the correlation function of positions and time lapse δt=0.1 and 1 s.

Note that the trajectories recorded provide only the nodes visited and the time elapsed between visits. The intermediate positions in the bonds between the nodes are needed for the calculation of the flow propagator. They are extrapolated by assuming that the velocity during the hop from one node to another is constant. Thus the trajectories consist of a continuous description of the position of the particles. This linear approximation will be discussed in Sec. IV.

Figures 5 and 6 show the flow propagator calculated for velocities $\langle v\rangle$=0.25, 1.25, and 3 mm/s, for δt=0.1 and 1 s. Note that the displacements are normalized by the mean displacement for clarity.

Qualitative features listed below that are observed experimentally [1–4,7,8] or numerically [5,31] are successfully reproduced in these figures.

For δt=0.1 s, the diffusion length is small ($\sqrt{D\delta t}\sim15$ μm). At low velocity $\langle v\rangle$=0.25 mm/s, the effect of diffusion can be observed and the left tail shows negative displacement. Note that part of the left tail is due to bond orientation. The long right tail evidences that some particles followed faster paths. At an average velocity of $\langle v\rangle$=3 mm/s, two peaks are observed. The separation of two peaks evidences the coexistence of slow or no flow zones with higher velocity paths. Time is too short to allow diffusion between those two zones. Note that there is no bump on the right tail, as sometimes observed experimentally [5]. This is due to the assumption of volumeless nodes [30]. At δt=1 s, particles will diffuse over a length scale $\sqrt{D\delta t}$ of the order of half a bond. At high velocity, although it is less

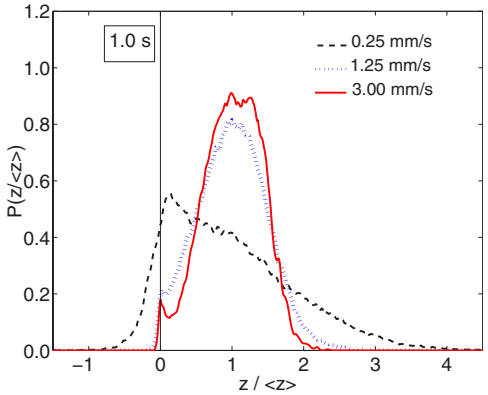

FIG. 6. (Color online) Flow propagator for an average velocity in the network $\langle v\rangle$=0.25, 1.25, and 3 mm/s and a time lapse δt=1 s.

marked, there is a separate peak at $z=0$ showing that the time is not sufficient to allow diffusion of particles out of slow flow zones. At very long times, as the medium is periodic in the direction of the flow, the particles will have totally probed the porous space and the distribution will tend to a Gaussian shape. The time needed for homogenization depends on the disorder of the medium and spatial correlation lengths; it is bounded by the time to diffuse over the cross section of the sample, that is, the ratio of the cross section to the diffusion coefficient ~ 3750 s. (This time scale is not measurable experimentally with NMR techniques.)

Note that this model describes only the spins that are actually detected, in other words, the particles represent the spins that have not relaxed during the time δt of the measurement. But the surface relaxation is faster than the bulk relaxation. Thus spins that spend time in bonds with smaller cross sections are more likely to relax. A correction to the current model can be added to calculate the resulting effect on the flow propagator.

We have provided here a method to calculate the flow propagator, and have shown two simple examples of the calculation. Systematic and quantitative comparison to experimental data on consistent networks will be reported in later presentations.

IV. DISCUSSION

Several assumptions were made to derive a simple approach. In this section, the limits of the model are detailed and corrections to the model are proposed when possible. We start with a technical point and then describe more general assumptions.

In this presentation of the model, the flow in every bond is described by a mean velocity. Depending on the case, this assumption is either valid, or can be corrected, or cannot hold. Let us consider a bond ij of cross section S_{ij}, mean velocity u_{ij}, and length l_{ij}. In a two-dimensional description, the local Péclet number is defined as $\wp l_{ij}=u_{ij}\sqrt{S_{ij}}/D_m$. D_m is the molecular diffusion (note that this definition differs from the definition used previously in the one-dimensional description of the flow). At low local Péclet numbers, transport is dominated by diffusion, that is, the particles probe all the flow lines of the cross section and thus have an equivalent mean velocity. The approximation is valid and the model does not need to be refined. At high local Péclet numbers, advection by the flow dominates. If the particles spend in the bond ij a time $t \gg S_{ij}/D$, they spend enough time in the bond to probe the cross section. Then, the dispersion is effectively diffusive, with an effective diffusion coefficient $D_{\mathrm{eff}ij}=D_m(1+\kappa_{ij}\wp_{lij}^2)$, where κ_{ij} depends on the geometry of the cross section [32]. The analytical formula for the calculation of κ as a function of the cross sectional shape can be found in [33]. The time needed to cross the bond ij is $t \approx l_{ij}/u_{ij}$. Thus the dispersion will be effectively diffusive when $\wp l_{ij} \ll l_{ij}/\sqrt{S_{ij}}$, the local Péclet number is smaller than the aspect ratio of the bond. In that case, the model can be refined by replacing the thermal diffusion coefficient $D=D_m$ with an effective diffusion coefficient for every bond $D=D_{\mathrm{eff}ij}$. Last, at high local Péclet numbers, if $\wp l_{ij} \ll l_{ij}/\sqrt{S_{ij}}$ is not verified, the plug flow description in the bonds is not valid.

Second, a central assumption of the model is the full mixing at the nodes. A particle moves to a new bond independently of the bond it just crossed, and its position in the cross section of this bond. This assumption is common to most of the porous network models mentioned [4,17,18,21,22]. But it may be worth reconsidering revisiting it in light of comparisons with experiments.

Third, another common assumption of the models previously cited is volumeless nodes. Although their volumes do not affect the topology of the network, this assumption will prevent any quantitative comparison in a porous medium where the nodes have a significant volume. With the structure of the model, it seems possible to add a specific description of the dynamics of the particles in the nodes. This will be reported in a later presentation.

Fourth, when applying the method to the calculation of the flow propagator, the intermediate position of particles between nodes was linearly approximated. Diffusion will cause particles to wander at the entrance of bonds that they do not cross, and wander within the bonds that are crossed. The efficiency of the continuous time random walk is due to the fact that this wandering is not detailed and is simply averaged in the distribution of times needed to go through each bond. The linear approximation induces a bias when trajectories are shorter that a bond length. Still, when considering an ensemble of particles distributed in bonds, it is a reasonable estimation of the average displacement. If an exact detailed expression is needed for very short distances or times, a simple random walk is better adapted than the continuous time random walk. Note that this is a negligible effect when trajectories longer than a single bond length are considered.

V. CONCLUSION

In this paper, we have presented an efficient method to calculate the trajectories of particles subject to advection and diffusion in disordered networks.

The method is computationally efficient and well adapted to large and heterogeneous networks. It is general and can be used for dispersion of passive or chemically active tracers in heterogeneous porous media. In this paper, it is applied to the calculation of the flow propagator in a network with a topology extracted from Berea sandstone. Qualitative features observed experimentally were reproduced. The domain of validity of the model and possible improvements are detailed in Sec. IV. Further work is currently ongoing to compare the calculated flow propagator with corresponding experimental data. The model can then be a powerful tool to understand the interplay between the structure of a porous medium and the dispersion in it [34].

ACKNOWLEDGMENTS

The authors wish to thank Claude Signer and Jefferson Tester for their constant support during this work, L.

Schwartz and P. Ganguli for careful rereading, and Martin Blunt for interesting discussions.

APPENDIX: INVERSE LAPLACE TRANSFORM OF THE FIRST ARRIVAL TIME DISTRIBUTION

The first arrival time distribution for a particle crossing bond ij was calculated in the Laplace domain as expressed in Eq. (6). Inverting the Laplace transform with standard general methods is very time consuming and cannot be performed for every bond if the size of the network is large. A specific analysis of the FATD is proposed whereby an approximation is used in the real time domain that enables fast computation.

The expression of $\tilde{p}_{ij}(s)$ in the Laplace domain reads

$$\tilde{\xi}_i^{-1}(s) = \sum_{k=1}^{z} S_{ik} \frac{\gamma_{ik}}{\tanh(\gamma_{ik} l_{ik})} \tag{A1}$$

$$\tilde{p}_{ij}(s) = S_{ij} \tilde{\xi}_i(s) \frac{-\gamma_{ij}}{e^{-\varphi_{ij}/2}[\sinh(\gamma_{ij} l_{ij})]} \tag{A2}$$

with $\gamma_{ij} = (1/2D)\sqrt{(u_{ij}^2 + 4Ds)}$.

In the time domain, the first arrival time distribution for a particle crossing bond ij is written

$$p_{ij}(t) = \frac{1}{2\pi i} \int_{s_0 - i\infty}^{s_0 + i\infty} e^{st} \tilde{p}_{ij}(s) ds, \tag{A3}$$

where s_0 is a real number greater than the real part of all the poles of the function $\tilde{p}_{ij}$.

The function $\tilde{p}_{ij}(s)$ is analytical in the complex plane except at the poles y_l, such that $\tilde{\xi}_i^{-1}(y_l) = 0$. [It is checked that $\tilde{p}_{ij}(s)$ is defined and differentiable for $x_n = -u_{ij}^2/4Dl - D(n\pi/l)^2$ with $n \in Z^+$].

Therefore the residues theorem is applied to calculate the integral (A3) and invert the Laplace transform:

$$p_{ij}(t) = \sum_{l=1}^{\infty} \mathrm{Res}(y_l). \tag{A4}$$

In the next section, the poles y_l, $l = 1, \ldots, \infty$, are identified. Their residues are then calculated. Note that the sum converges reasonably fast and can therefore be truncated to estimate the numerical expression of $p_{ij}(t)$.

Calculation of the poles

The function is analytical in the complex plane, but at the poles y_l, $l = 1, \ldots, \infty$, such that

$$\tilde{\xi}_i^{-1}(y_l) = 0, \quad \text{that is,} \quad \sum_{k=1}^{z} S_{ik} \frac{(1/2D)\sqrt{(u_{ik}^2 + 4Dy_l)}}{\tanh[(l_{ik}/2D)\sqrt{(u_{ik}^2 + 4Dy_l)}]} = 0. \tag{A5}$$

We thus look for the roots of the complex function $\xi_i^{-1}(y)$. The function is a sum of functions of the type

$$f(y) = \begin{cases} \dfrac{\sqrt{u^2 + 4Dy}}{\tanh\left(\dfrac{l}{2D}\sqrt{(u^2 + 4Dy)}\right)} & \text{if } y > -\dfrac{u^2}{4D}, \\ \dfrac{\sqrt{u^2 + 4Dy}}{\tan\left(\dfrac{l}{2D}\sqrt{(u^2 + 4Dy)}\right)} & \text{if } y < -\dfrac{u^2}{4D} \end{cases}. \tag{A6}$$

The function f is strictly monotonic and has poles in the real space at $x_n = u^2/4Dl - D(n\pi/l)^2$ with $n \in Z_+^*$. The limits of f at each pole are such that

$$\lim_{y \to x_n^-} f(y) = +\infty \quad \text{and} \quad \lim_{y \to x_n^+} f(y) = -\infty. \tag{A7}$$

The function ξ_i^{-1} is a sum of functions of type f. Therefore it has an infinite number of poles $x_n^{ij} = u_{ij}^2/4Dl - D(n\pi/l)^2$, with $n \in Z_+^*$ and $j \in [1, z]$. The poles are ordered and labeled w_n with $n \in Z_+$ (w_0 is set to zero). The function ξ_i^{-1} is strictly monotonic in every interval $[w_n, w_{n+1}]$, with limits

$$\lim_{y \to w_n^+} \xi_i^{-1}(y) = -\infty \quad \text{and} \quad \lim_{y \to w_{n+1}^-} \xi_i^{-1}(y) = -\infty. \tag{A8}$$

Each root y_l of ξ_i^{-1} is bracketed by consecutive poles w_n, w_{n+1}. It is thus efficiently calculated with a standard gradient method.

Calculation of the residues

The residues are calculated using the relation

$$\mathrm{Res}(y_l) = \frac{-\dfrac{1}{2D}\sqrt{(u_{ij}^2 + 4Dy_l)}}{e^{-\varphi_{ij}/2}\left[\sinh\left(\dfrac{1}{2D}\sqrt{(u_{ij}^2 + 4Dy_l)} l_{ij}\right)\right]} \frac{e^{y_l t}}{\xi^{-1}(y_l)'}. \tag{A9}$$

The first arrival time distribution to cross bond ij is then calculated by summing the residues:

$$p_{ij}(t) = \sum_{l=1}^{\infty} \mathrm{Res}(y_l). \tag{A10}$$

The convergence of the sum is fast, and generally requires a limited number of terms. Still, it is more subtle for very short times. Slower convergence can be worked out because it occurs in ranges where p_{ij} is negligible.

[1] P. T. Callaghan and Y. Xia, Science **90**, 177 (1991).
[2] J. D. Seymour and P. T. Callaghan, AIChE J. **43**, 2096 (1997).
[3] M. H. G. Amin, S. J. Gibbs, R. J. Chorley, K. S. Richards, T. A. Carpenter, and L. D. Hall, Proc. R. Soc. London, Ser. A **453**, 489 (1997).
[4] L. Lebon, L. Oger, J. Leblond, J. P. Hulin, N. S. Marysand, and L. M. Schwartz, Phys. Fluids **8**, 293 (1996).
[5] L. Lebon, J. Leblond, and J. P. Hulin, Phys. Fluids **9**, 481 (1997).
[6] U. M. Scheven and P. N. Sen, Phys. Rev. Lett. **89**, 254501 (2002).
[7] U. M. Scheven, D. Verganelakis, R. Harris, M. L. Johns, and L. F. Gladden, Phys. Fluids **17**, 117107 (2005).
[8] P. Singer, G. Leu, E. J. Fordham, and P. Sen, J. Magn. Reson. **183**, 167 (2006).
[9] J. J. Tessier and K. J. Packer, Phys. Fluids **10**, 75 (1998).
[10] C. P. Lowe and D. Frenkel, Phys. Rev. Lett. **77**, 4552 (1996).
[11] B. Berkowitz, H. Scher, and S. E. Silliman, Water Resour. Res. **36**, 149 (2000).
[12] B. Berkowitz, A. Cortiz, M. Dentzand, and H. Scher, Rev. Geophys. **44**, RG2003 (2006).
[13] R. Al-Raousha, K. Thompson, and C. S. Willson, Soil Sci. Soc. Am. J. **67**, 1687 (2003).
[14] P. E. Oeren and S. Bakke, J. Pet. Sci. Eng. **39**, 177 (2003).
[15] P. H. Valvatne and M. J. Blunt, Water Resour. Res. **40**, W07406 (2004).
[16] R. M. Sok, M. A. Knackstedt, A. P. Sheppard, A. P. Pinczewski, W. B. Lindquist, A. Venkatarangan, and L. Paterson, Transp. Porous Media **46**, 345 (2002).
[17] K. S. Sorbie and P. J. Clifford, Chem. Eng. Sci. **46**, 2525 (1991).
[18] R. A. Damion, K. J. Packer, K. S. Sorbie, and S. R. McDougall, Chem. Eng. Sci. **55**, 5981 (2000).
[19] C. Bruderer and Y. Bernabé, Water Resour. Res. **37**, 897 (2001).
[20] C. Bruderer-Weng, P. Coiwe, Y. Bernabé, and Y. Main, Adv. Water Resour. **27**, 843 (2004).
[21] B. Bijeljic, A. H. Muggeridge, and M. J. Blunt, Water Resour. Res. **40**, W11501 (2004).
[22] M. E. Rhodes and M. J. Blunt, Water Resour. Res. **42**, W04501 (2006).
[23] L. deArcangelis, J. Koplik, S. Redner, and D. Wilkinson, Phys. Rev. Lett. **57**, 996 (1986).
[24] J. Koplik, S. Redner, and D. Wilkinson, Phys. Rev. A **37**, 2619 (1988).
[25] K. C. Loh and A. Geng, Chem. Eng. Sci. **58**, 3439 (2003).
[26] B. Bijeljic and M. J. Blunt, Water Resour. Res. **42**, W01202 (2006).
[27] P. H. Valvatne, Ph.D., Department of Earth Science and Engineering, Imperial College, 2003.
[28] J. P. Bouchaud and A. Georges, Phys. Rep. **195**, 127 (1990).
[29] S. Redner, *A Guide to First Passage Processes* (Cambridge University Press, Cambridge, U.K., (2001).
[30] R. Duplay and P. N. Sen, Phys. Rev. E **70**, 066309 (2004).
[31] B. Manz, L. F. Gladden, and P. B. Warren, AIChE J. **45**, 1845 (1999).
[32] G. Taylor, Proc. R. Soc. London, Ser. A **219**, 186 (1953).
[33] R. Aris, Proc. R. Soc. London, Ser. A **235**, 67 (1956).
[34] D. Kandhai, D. Hlushkou, A. G. Hoekstra, P. M. A. Sloot, H. Van As, and U. Tallarek, Phys. Rev. Lett. **88**, 234501 (2002).